Enhanced Efficiency of Single and Tandem Organic Solar Cells Incorporating a Diketopyrrolopyrrole-Based Low-Bandgap Polymer by Utilizing Combined ZnO/Polyelectrolyte Electron-Trans...

ARTICLE *in* ADVANCED MATERIALS · SEPTEMBER 2013

Impact Factor: 17.49 · DOI: 10.1002/adma.201301288 · Source: PubMed

10 AUTHORS, INCLUDING:

Samuel D Collins
University of California, Santa Barbara
12 PUBLICATIONS **343** CITATIONS
SEE PROFILE

Jin Young Kim
Ulsan National Institute of Science and Tec...
496 PUBLICATIONS **9,021** CITATIONS
SEE PROFILE

Thanh Luan Nguyen
Pusan National University
14 PUBLICATIONS **221** CITATIONS
SEE PROFILE

Mario Leclerc
Laval University
223 PUBLICATIONS **18,473** CITATIONS
SEE PROFILE

Enhanced Efficiency of Single and Tandem Organic Solar Cells Incorporating a Diketopyrrolopyrrole-Based Low-Bandgap Polymer by Utilizing Combined ZnO/Polyelectrolyte Electron-Transport Layers

Jang Jo, Jean-Rémi Pouliot, David Wynands, Samuel D. Collins, Jin Young Kim, Thanh Luan Nguyen, Han Young Woo, Yanming Sun, Mario Leclerc, and Alan J. Heeger**

Solution-processed bulk heterojunction (BHJ) organic solar cells based on conjugated polymer:fullerene composites have attracted considerable attention in both academia and industry due to their low cost, relative ease of fabrication and the potential for use in flexible devices.[1] Research efforts have developed higher efficiency solar cells using various strategies, such as morphology engineering (e.g., thermal/solvent annealing, and processing additives),[2] interface engineering (e.g., anode/cathode interfacial layers)[3] and materials innovation (e.g., novel donor/acceptor materials).[4] Recently, encouraging power conversion efficiencies (PCEs) of 9.2% have been reported for single BHJ polymer solar cells.[5] However, compared with polycrystalline silicon-wafer-based solar cells, the efficiency is still relatively low, primarily because of the relatively narrow absorption window for most low-bandgap conjugated polymers. By carefully tuning the backbone, the side chains and the substituents of conjugated polymers, their spectral response can be extended to the near-infrared region (≈1100 nm). The corresponding solar cells tend to have low open-circuit voltage (V_{oc}), however, limiting the further improvement in PCE.[6] In addition, significant energy losses are unavoidable for single BHJ organic solar cells, as photons with energy smaller than the bandgap are not absorbed, while photons with energy larger than the bandgap are absorbed, but the excess energy is lost by thermalization.[7]

Tandem device architectures have been demonstrated as a useful approach towards fabrication of high-efficiency solar cells, where two subcells are stacked in series and the individual photoactive layers have complementary absorption spectra.[8] This tandem configuration can address the limitations of single BHJ organic solar cells because a broader spectrum of solar radiation can be covered. Furthermore, thermalization losses are reduced, since high energy photons are converted by the large bandgap subcell, providing a high V_{oc}, while low energy photons are converted by the low bandgap subcell at a lower V_{oc}. The V_{oc} of an optimized tandem cell is the sum of V_{oc} of the individual subcells. According to the simulated results by Dennler et al., PCE as high as 15% can be achievable for a polymer tandem cell with optimized materials combination.[9] PCEs over 10% have been recently reported for both polymer tandem cells and vacuum-processed small-molecule tandem cells, showing that the tandem structure provides a very promising route to enable the development of high-efficiency organic solar cells.[10]

As noted above, in a tandem cell, a low bandgap (E_g = 1.2–1.5 eV) polymer is needed to absorb longer-wavelength photons, which can generate a large short-circuit current density (J_{sc}). On the other hand, the energy level of low-bandgap materials must be well designed to ensure efficient charge separation and to obtain large V_{oc}. However, most low-bandgap materials reported in the literature have either large J_{sc} and low V_{oc}, or large V_{oc} and low J_{sc}, resulting in a moderate PCE (<7%).[6] The lack of high-performance low-bandgap materials has been identified as a major limiting factor for achieving high-performance solution-processed tandem organic solar cells.

Recently, diketopyrrolopyrrole (DPP)-based materials have been attracting interest for application in organic solar cells.[11] The strong electron-deficient nature of DPP unit makes it a promising building block to construct low-bandgap conjugated polymers. PCEs of DPP-based low-bandgap polymers over 6% and 8.6% have been recently reported in single and tandem organic solar cells, respectively.[11b,12]

In this contribution, we introduce a DPP-based low bandgap (E_g ≈ 1.49 eV) polymer, poly[{2,5-bis(2-octyldodecyl)-2,3,5,6-tetrahydro-3,6-dioxopyrrolo[3,4-c]pyrrole-1,4-diyl}-alt-{[2,2′-(1,4-phenylene)bisthiophene]-5,5′-diyl}] (PDPPTPT). This material has been reported previously, but only with moderate PCE

Dr. J. Jo, Dr. D. Wynands, S. D. Collins, Dr. Y. Sun, Prof. A. J. Heeger
Center for Polymers and Organic Solids
University of California
Santa Barbara, California 93106, USA
E-mail: sunym@iccas.ac.cn; ajhe1@physics.ucsb.edu
J.-R. Pouliot, Prof. M. Leclerc
Department of Chemistry
Université Laval
Quebec City, QC, G1V 0A6, Canada
Prof. J. Y. Kim
Interdisciplinary School of Green Energy
Ulsan National Institute of Science and Technology (UNIST)
Ulsan 689-798, South Korea
T. L. Nguyen, Prof. H. Y. Woo
Department of Cogno-Mechatronics Engineering (WCU)
Pusan National Unisversity
Miryang 627-706, South Korea

DOI: 10.1002/adma.201301288

(≈5.5%).[13] Here, we demonstrate that PCEs of more than 7% can be achieved in single BHJ organic solar cells with an inverted device structure that comprises a high-molecular-weight PDPPTPT as the donor and [6,6]-phenyl C_{71}-butyric acid methyl ester ($PC_{70}BM$) as the acceptor by using multiple approaches to optimize the device. Firstly, during solution process, an additive mixture consisting of 1,8-diiodooctane (DIO) and 1-chloronaphthalene (CN) was incorporated into the chlorobenzene (CB) host solvent to optimize the BHJ nanomorphology and thus to improve the cell performance. Secondly, an ultrathin conjugated polyelectrolyte (CPE) layer was employed between the ZnO and BHJ layers to improve the electron transport and interfacial contact. Compared with cells fabricated with bare ZnO layer, the J_{sc} increased by 11% (from 13.11 to 14.54 mA cm^{-2}) for device with ZnO/CPE layer, while maintaining high V_{oc} of 0.78 V, and thus PCE over 7% was achieved. This is among the highest values reported for DPP-based single BHJ organic solar cells.[14] Finally, we demonstrate that after incorporating a wide-bandgap ($E_g \approx 1.8$ eV) polymer, thieno[3,4-c]pyrrole-4,6-dione (TPD)-terthiophene copolymer (P2), as a front cell, and ZnO/CPE layer as electron-transport layers into tandem solar cells, the devices achieve PCEs of ≈8.6%, with J_{sc} of 8.36 mA cm^{-2}, V_{oc} of 1.60 eV, and fill factor (FF) of 64%. The results show that PDPPTPT is an ideal low-bandgap polymer to make high-efficiency solution-processed tandem organic solar cells. Moreover, the results show that the interfacial engineering of the charge-carrier transport layer is a useful approach to further improving the PCEs of tandem organic solar cells.

Figure 1a shows the device structure of the single BHJ polymer solar cells, together with the molecular structures of PDPPTPT, $PC_{70}BM$ and the conjugated polyelectrolyte (CPE), poly(9,9′-bis(6″-N,N,N-trimethylammoniumhexyl) fluorene-co-alt-phenylene) with bromide counterions (FPQ-Br). Solar cells are fabricated in the inverted structure, where sol-gel-derived ZnO film has been used as the electron-transport layer. A detailed description of the device fabrication is available in the Experimental Section. PDPPTPT was synthesized by a Suzuki cross coupling reaction (see Supporting Information). The UV–vis absorption spectra of the films of PDPPTPT and P2 along with the solar radiation spectrum are shown in Figure 1b. The optical bandgap of PDPPTPT was determined from the onset (≈830 nm) of the absorption spectrum at ≈1.49 eV.

Incorporating solvent additives into the solutions from which the BHJ layers are cast is widely used for the fabrication of high-performance BHJ organic solar cells.[2d,e] Typically, the solvent additives should have a higher boiling point (b.p.) than that of the host solvent as it can allow polymers or fullerenes to have a relatively long period to self-organize, which induces nanometer-scale phase-separated morphology of the BHJ films, hence leading to better solar cell performance. In this contribution, we used chlorobenzene (b.p. = 132 °C) as the host solvent to dissolve PDPPTPT polymer (M_n = 29 kDa; PDI = 3.04). The other two solvents, DIO (b.p. = 332.5 °C) and CN (b.p. = 259 °C) were chosen as processing additives.

The current density–voltage (*J–V*) characteristics of the solar cells measured under simulated AM 1.5 G irradiation (with intensity of 100 mW cm^{-2}) are shown in **Figure 2**. The device performance is summarized in **Table 1**. A PCE of 3.4% was achieved for solar cells fabricated with CB/CN (97:3 v/v)

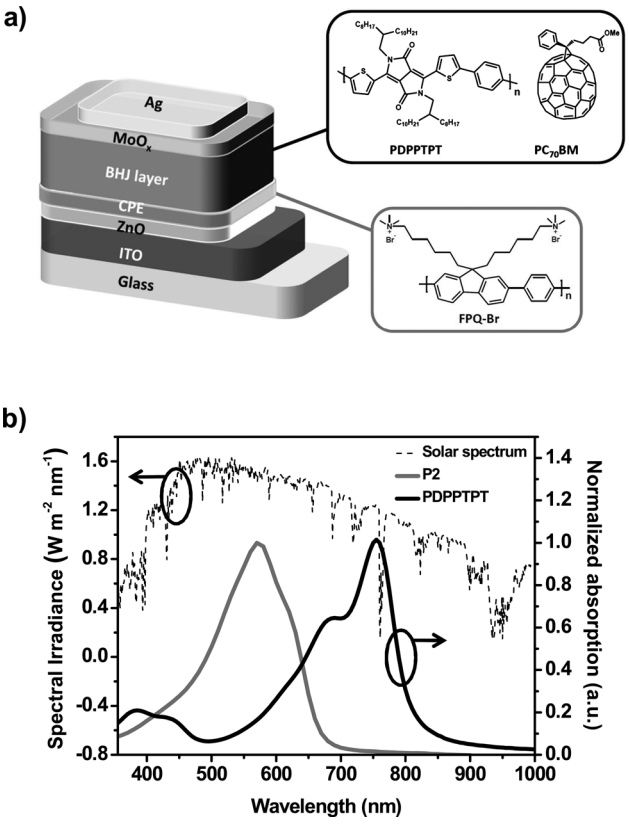

Figure 1. a) Device structure of polymer solar cells with an inverted architecture and molecular structures of PDPPTPT, $PC_{70}BM$ and CPE. b) UV–vis absorption spectra of PDPPTPT, P2, as well as the solar radiation spectrum.

solvent, which is lower than that (≈4.6%) of cells using CB/DIO (97:3 v/v) solvent. By using a ternary solvent mixture, we find that the cell performance can be dramatically improved. While keeping the content of CN at 3% by volume and increasing

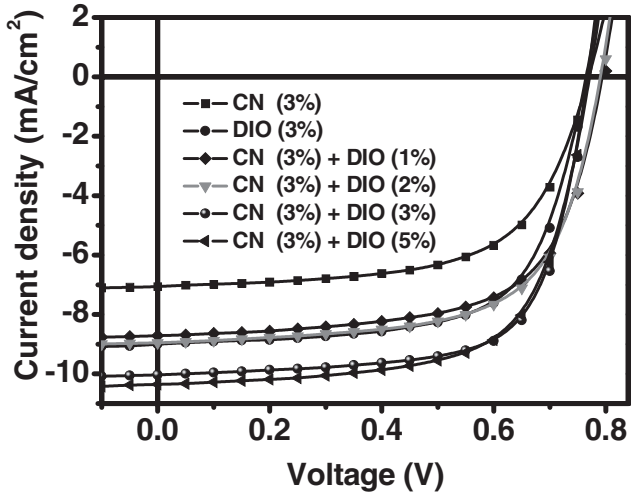

Figure 2. *J–V* characteristics of single BHJ solar cells based on low-MW PDPPTPT:$PC_{70}BM$ blend films processed with various volume ratios of DIO and CN additive mixtures, where chlorobenzene is used as the host solvent.

Adv. Mater. **2013**,
DOI: 10.1002/adma.201301288

Table 1. Summary of the performances of single BHJ solar cells based on PDPPTPT:$PC_{70}BM$ blend films processed from different additive mixtures and a combination of ZnO/CPE layer.

Addtives		V_{oc} [V]	J_{sc} [mA cm^{-2}]	FF [%]	PCE [%]
CN	DIO				
3%	0%	0.77	7.1	63	3.40
0%	3%	0.77	9.0	66	4.57
3%	1%	0.80	8.7	65	4.49
3%	2%	0.79	9.0	65	4.63
3%	3%	0.77	10.0	69	5.34
3%	3%	0.78	13.4	63	6.37[a)]
3%	3%	0.78	14.5	62	7.04[b)]
3%	5%	0.77	10.4	67	5.32

[a)]Solar cells based on high-MW PDPPTPT:$PC_{70}BM$ blend films without a CPE layer; [b)]Solar cells based on high-MW PDPPTPT:PC70BM blend films with CPE layer.

the DIO volume from 1% to 3% in the solvent mixture, J_{sc} is increased steadily from 8.7 to 10 mA cm^{-2} with little change in either the V_{oc} or the FF. As a result, the overall efficiency is improved from ≈4.5 to 5.3%. Afterwards, the devices show a minor drop in efficiency on further increasing the amount of DIO additive because of a reduction in FF. The optimal ratio of the ternary solvent mixture is CB/DIO/CN = 94:3:3 by volume, with the peak efficiency of ≈5.3%. Considering the difference in selective solubility of the additives, DIO may contribute to form well-defined interface between donor:acceptor nanophases. Both cases of using binary mixtures with CB/DIO or CB/CN solvent resulted in a lower efficiency. The mechanism of the role of three combined solvents associated with the improved device performance is poorly understood at this stage and needs further investigation.

We note that solar cell performance is strongly dependent on the molecular weight (MW) of the PDPPTPT polymer. Under nearly identical processing conditions (e.g., same ratio of the ternary solvent mixture mentioned above), a PCE of ≈6.4% has been obtained when a high-MW version of PDPPTPT (M_n = 108 kDa; PDI = 2.72) is used. The efficiency improvement is primarily attributed to the improvement in J_{sc} (by ≈11%) (**Figure 3**a). A combination of CPE and titanium oxide (TiO_x) has been previously demonstrated as an effective approach to improve the interfacial contact between the active layer and ITO electrode.[15] In this work, the CPE has been employed to modify the ZnO layer. After surface modification by using the ultrathin CPE layer, the ZnO film becomes smoother (Figure S1) and the work function is reduced from ≈4.7 eV to ≈4.1 eV, which facilitates electron transport from BHJ photoactive layer to the ITO electrode. We note that the combination of ZnO/CPE layer in high-MW PDPPTPT based solar cells further enhances the efficiency. The resulting device exhibits V_{oc} = 0.78 V, J_{sc} = 14.5 mA cm^{-2}, and FF = 62%, with the overall efficiciency of ≈7.04%. This value is among the highest reported for DPP-based single polymer solar cells.

The incident photon-to-current-conversion efficiency (IPCE) spectra of solar cells fabricated with or without CPE are displayed in Figure 3b. Obvious IPCE enhancements in solar cells

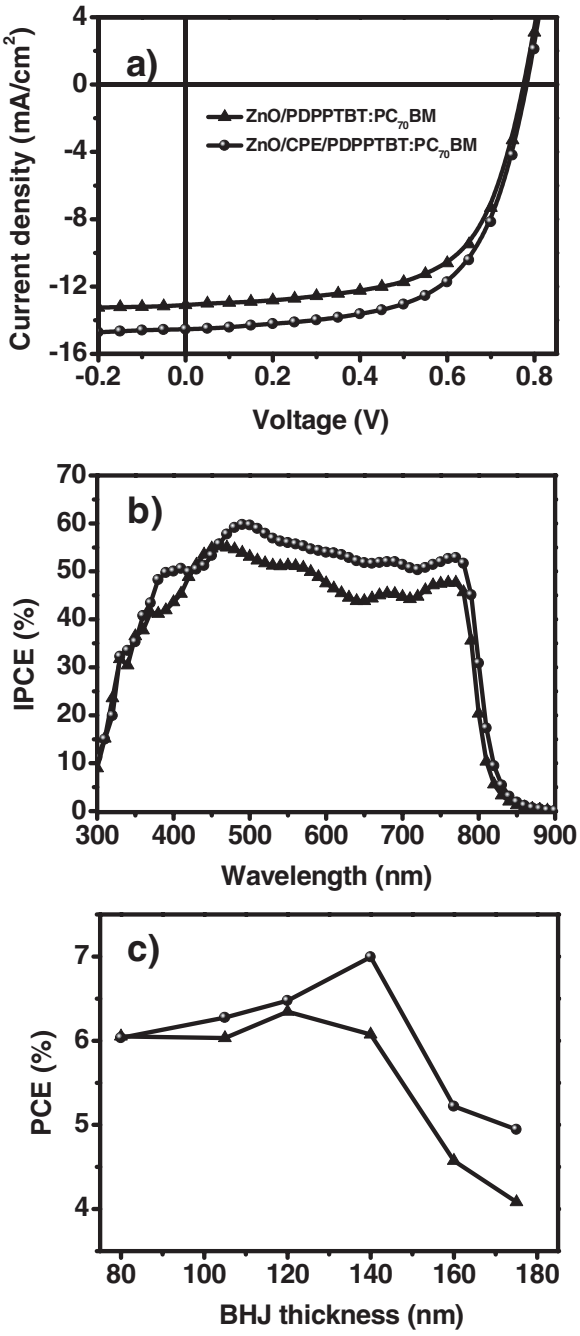

Figure 3. a) *J–V* characteristics and b) IPCE spectra of single BHJ solar cells based on high-MW PDPPTPT:$PC_{70}BM$ blend films with and without CPE layer. c) PCEs of solar cells with a function of BHJ photoactive layer thickness.

fabricated with CPE layer in the wavelength range from 400 nm to 800 nm can be clearly seen: the average IPCE peak in the visible region is over 50% (the maximum peak is 60% at 500 nm), in a good agreement with the observed J_{sc} (14.5 mA cm^{-2}). The device performance as a function of BHJ photoactive layer thickness was also investigated. As shown in Figure 3c, the best device with 7% efficiency had a BHJ layer thickness of ≈140 nm. The devices show a drop in efficiency on further

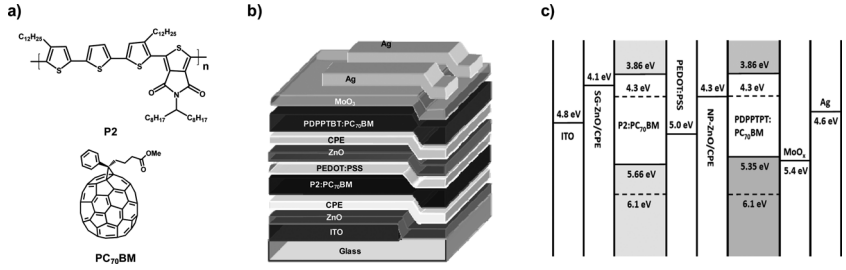

Figure 4. a) Molecular structures of wide-bandgap material, P2 and $PC_{70}BM$. b) Device structure of tandem solar cells. c) Schematic energy level diagrams of tandem organic solar cells.

increasing the thickness. The efficiency is decreased below 5% at the BHJ layer thickness of ≈175 nm.

On the basis of the single device results, PDPPTPT exhibits great potential for making tandem solar cells. Typically, large-bandgap polymers, such as poly(3-hexylthiophene) (P3HT) and poly[N-9″-hepta-decanyl-2,7-carbazole-*alt*-5,5-(4′,7′-di-2-thienyl-2′,1′,3′-benzothiadiazole)] (PCDTBT) have been used in the fabrication of high efficiency tandem cells.[8e,10,12b] Here, we introduce another large-bandgap material (P2, **Figure 4**a), which has shown excellent performance with J_{sc} over 10 mA cm^{-2}, high V_{oc} = 0.92 V, as well as high FF = 63%.[16] The P2 absorption spectrum is shown in Figure 1b. Combined with the PDPPTPT, these two polymers exhibit complementary absorption spectra from 350 nm to 850 nm. The absorption spectra of polymers with fullerene films were also measured (Supporting Information, Figure S2). The tandem cell structure and the corresponding energy level diagram are shown in Figure 4b,c. Sol-gel-derived (SG) ZnO and ZnO nanoparticles (NP) have been used as the electron-transport layers in the front and rear subcells, respectively.[17] The reason why NP-ZnO was chosen as the electron-transport layer in the rear cell is due to its relatively low annealing temperature (≈80 °C), which does not affect a change of BHJ nanomorphology in the front cell. The work functions of the different ZnO films are all ≈4.7 eV, determined by Kelvin Probe measurements, and an ultrathin CPE layer (<10 nm) has been used to modify the ZnO layers. Three different multistacked tandem solar cells were fabricated:

(A) ITO/SG-ZnO/P2:$PC_{70}BM$/PEDOT:PSS/NP-ZnO/PDPPTPT:$PC_{70}BM$/MoO_x/Ag;
(B) ITO/SG-ZnO/P2:$PC_{70}BM$/PEDOT:PSS/NP-ZnO/CPE/PDPPTPT:$PC_{70}BM$/MoO_x/Ag;
(C) ITO/SG-ZnO/CPE/P2:$PC_{70}BM$/PEDOT:PSS/NP-ZnO/CPE/PDPPTPT:$PC_{70}BM$/MoO_x/Ag;

J–V curves of the single BHJ solar cells and the three different tandem solar cells are displayed in **Figure 5**. Compared with device A, device B resulted in increased J_{sc}, FF, and consequently enhanced PCE. Furthermore, device C incorporating CPE layers both in the front and rear cells exhibited the best PCE of around 8.6% (the average PCE from eight individual devices is 8.39%). A summary of the solar cell performance data is given in **Table 2**.

The V_{oc} value of the device A is close to the sum of V_{oc} of the two subcells, indicating that poly(3,4-ethylenedioxythiophene):poly(styrene sulfonate)/ZnO nanoparticles (PEDOT:PSS/NP-ZnO) acts as an excellent interconnection layer in tandem solar cells. The CPE modification not only smoothes the surface of NP-ZnO films (Supporting Information, Figure S1), but also decreases the work functions from ≈4.7 eV to ≈4.3 eV. The decreased work function reduces the energy barrier between PDPPTPT:$PC_{70}BM$ layer and ZnO, which enables it more efficiently to collect the electrons, therefore enhancing the device performance (device B and C) in comparison with device A. SG-ZnO layer modified by CPE layer also facilitates electron transport between P2:$PC_{70}BM$ active layer and ITO electrode, yielding the best performance for device C. These results show that PDPPTPT is an excellent low-bandgap material for efficient tandem solar cells. Moreover, the results show that the modification of electron-transport layers used both in the front and rear cells (for inverted tandem structure) is a useful approach to further improve the PCEs of organic tandem solar cells. Note that the high-performance solution-processed tandem solar cells reported in the literature were fabricated with PEDOT:PSS/NP-ZnO as the interconnection layer (without any surface modification). Higher efficiencies are expected if appropriate interfacial engineering is employed.

In conclusion, single BHJ solar cells based on a DPP-based low-bandgap polymer, PDPPTPT, have been fabricated. Multiple approaches have been employed to optimize the device, including a ternary solvent mixture to dissolve PDPPTPT:$PC_{70}BM$ BHJ materials and a combination of CPE and ZnO as the electron-transport layer. A high efficiency, PCE = 7.04%, has been achieved, which is among the highest values reported for DPP-based single polymer solar cells. Furthermore, after incorporating a wide-bandgap polymer (P2) and ZnO/CPE layer into the series-connected tandem structure, the devices exhibited PCEs of approximately 8.6%, indicating that

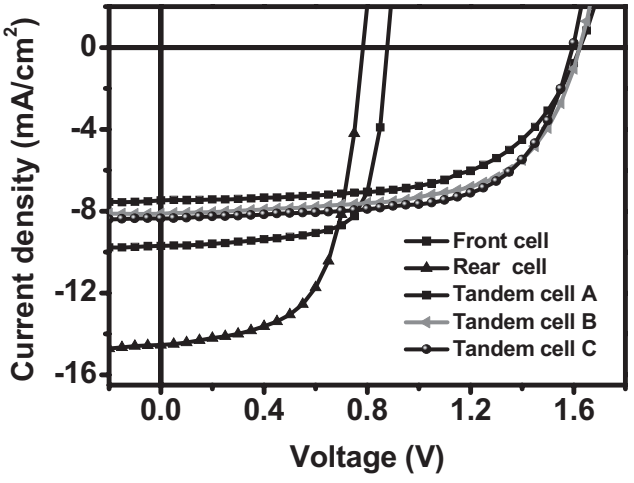

Figure 5. *J–V* characteristics of single cells based on P2:$PC_{70}BM$ and PDPPTPT:$PC_{70}BM$ BHJ films, and tandem solar cells fabricated with and without CPE layer between ZnO and BHJ layers.

Adv. Mater. **2013**,
DOI: 10.1002/adma.201301288

Table 2. Single and tandem solar cell performances.

Device structure	V_{oc}[a)] [V]	J_{sc}[a)] [mA cm^{-2}]	FF[a)] [%]	PCE[a)] [%]
Front cell	0.88	9.7	73	6.18
Rear cell	0.78	14.5	62	7.04
Tandem solar cell A	1.62	7.5	60	7.23
Tandem solar cell B	1.61	8.0	62	8.04
Tandem solar cell C	1.60 (1.61)	8.4 (8.3)	64 (63)	8.58 (8.39%)

[a)]The values in parentheses are average values from eight individual devices.

PDPPTPT is an excellent low-bandgap material for the fabrication of high-efficiency solution-processed tandem solar cells. The interfacial engineering plays an important role in obtaining high performance organic tandem devices.

Experimental Section

Preparation of the ZnO Films: The synthesis of SG-ZnO has been reported by Sun et al.[17a] ZnO nanoparticles are synthesized according to Beek et al.[17b]

Fabrication of Single BHJ Solar Cells: All the devices were fabricated onto transparent indium tin oxide (ITO)-coated glass substrates that were pre-cleaned with detergent and by ultrasonication sequentially with deionized (DI) water, acetone, and isopropyl alcohol. After complete drying in a high-temperature oven, ZnO precursor solution was spin-cast onto the ITO substrate (pretreated with UV-ozone for 15 min) and the SG-ZnO film was heated at 220 °C for 40 min in air. An ultrathin CPE layer (<10 nm) was also formed on the ZnO film by spin-coating with a solution (0.1 wt%) dissolved in solvent mixture composed of isopropyl alcohol and DI water (1:1 v/v) and the film was dried at 120 °C for 10 min. After transporting the films into a N_2-filled glovebox, a photoactive layer was deposited onto the film by spin-coating with a blend solution composed of PDPPTPT and $PC_{70}BM$ (1:2 wt/wt). The low-molecular-weight polymers were readily soluble in chlorobenzene (CB) solvent at a temperature below 60 °C, but the high-molecular-weight polymers were required to be processed from hot solution for the fabrication of high-quality films. For example, a hot solution (around 120 °C) of the PDPPTPT:$PC_{70}BM$ mixture dissolved in CB with processing additives (3% DIO and 3% CN by volume) was directly dropped and spin-cast onto the top of the ZnO/CPE layers. The film was then dried at 60 °C for 10 min. Finally, MoO_3 (≈5 nm) and Ag (≈100 nm) anodes were deposited on the active layers by a thermal evaporation method under high vacuum (<4×10^{-6} mbar; 1 mbar = 0.75 Torr) with a shadow mask. All the devices were encapsulated with a thin cover glass and a UV-curable epoxy in the N_2-filled glove box.

The *J–V* curves were measured using a Keithley 2400 SMU. The devices were illuminated through an aperture (11.8 mm^2) at an intensity of 100 mW cm^{-2} from a 1 kW solar simulator with an AM 1.5G filter in air. The IPCE spectra were measured with a QE measurement system (PV measurements, Inc.). A reference silicon photodiode traceable to NIST was used for monochromatic power-density calibrations.

Fabrication of Tandem Solar Cells: First, SG-ZnO/CPE layer was formed by the spin-coating method onto an ITO substrate in air before transporting the film into a N_2-filled glovebox for further device-fabrication processes. P2:$PC_{70}BM$ BHJ layer (≈80 nm) was deposited onto the SG-ZnO/CPE layers by spin-coating with blend solutions composed of P2 and $PC_{70}BM$ (15 mg each) dissolved in 1 mL of CB solvent with 3% CN by volume. The film was then dried at 60 °C for 10 min. PEDOT:PSS layer (60 nm) was deposited on the P2:$PC_{70}BM$ BHJ layer by spin-coating with Clevios CPP105D solution (filtered using a 5.0 µm Whatman Puradisc FP30 syringe filter), diluted with isopropyl alcohol at a 4:1 volume ratio. The film was then dried at 120 °C for 10 min in air. The NP-ZnO layer (≈35 nm) was deposited onto the PEDOT:PSS layer by spin-coating with ZnO nanoparticles dispersed in 2-methoxyethanol (15 mg/mL). The solution was applied to ultrasonication for 15 min prior to spin-coating deposition. The film was dried at 80 °C for 10 min in air. For the fabrication of the best-performing tandem device, an ultrathin CPE layer (<10 nm) was deposited onto the NP-ZnO film by spin-coating and dried at 120 °C for 10 min in air. After transporting the films into a N_2-filled glovebox, a hot solution (around 120 °C) of the PDPPTPT:$PC_{70}BM$ mixture (1:2 wt/wt) dissolved in CB with additive mixture (3% DIO and 3% CN by volume) was spin-cast onto the film, and the BHJ layer was dried at 60 °C for 10 min. MoO_3 (≈5 nm) and Ag (≈100 nm) were sequentially deposited on the film by thermal evaporation under high vacuum with a shadow mask. The *J–V* curves of the encapsulated tandem solar cells were measured using the same method as that for single device.

Kelvin Probe Measurements: Work-function values for ZnO and ZnO/CPE were measured under N_2 atmosphere (<3 ppm O_2) with a GB050 Scanning Kelvin Probe (KP Technology Ltd.), which utilized a stainless-steel probe, 2 mm in diameter, at a backing potential of ±7 V. Contact potential difference (CPD) values were determined from the average of 144 points taken over a 1.2 mm × 1.2 mm scan area (effective area probed was about 3 mm × 3 mm). CPD measurements determined in this way showed standard deviations of less than 13 meV. Work-function values were obtained by calibrating the probe against a freshly cleaved highly-ordered pyrolytic graphite (HOPG) sample, which was assumed to have a work-function value of 4.6 eV.[18]

Supporting Information

Supporting Information is available from the Wiley Online Library or from the author.

Acknowledgements

Research at UCSB including the fabrication and testing of solar cells and the measurements and analysis were supported by the Air Force Office of Scientific Research, (AFOSR FA9550-11-1-0063), Dr. Charles Lee, Program Officer. Research at Laval was partially supported by the NSERC PV network. H.Y.W. acknowledges the NRF grant (2012R1A1A2005855, R31-2008-000-20004-0) by the Ministry of Education, Science and Technology, Korea.

Received: March 21, 2013
Revised: April 30, 2013
Published online:

[1] a) G. Yu, J. Gao, J. C. Hummelen, F. Wudl, A. J. Heeger, *Science* **1995**, *270*, 1789; b) B. Kippelen, J. L. Bredas, *Energy Environ. Sci.* **2009**, *2*, 251; c) F. C. Krebs, *Sol. Energy Mater. Sol. C.* **2009**, *93*, 394.
[2] a) G. Li, V. Shrotriya, J. S. Huang, Y. Yao, T. Moriarty, K. Emery, Y. Yang, *Nat. Mater.* **2005**, *4*, 864; b) W. L. Ma, C. Y. Yang, X. Gong, K. Lee, A. J. Heeger, *Adv. Funct. Mater.* **2005**, *15*, 1617; c) G. Li, Y. Yao, H. Yang, V. Shrotriya, G. Yang, Y. Yang, *Adv. Funct. Mater.* **2007**, *17*, 1636; d) J. Peet, J. Y. Kim, N. E. Coates, W. L. Ma, D. Moses, A. J. Heeger, G. C. Bazan, *Nat. Mater.* **2007**, *6*, 497; e) J. K. Lee, W. L. Ma, C. J. Brabec, J. Yuen, J. S. Moon, J. Y. Kim, K. Lee, G. C. Bazan, A. J. Heeger, *J. Am. Chem. Soc.* **2008**, *130*, 3619.
[3] a) R. Steim, F. R. Kogler, C. J. Brabec, *J. Mater. Chem.* **2010**, *20*, 2499; b) H. Ma, H. L. Yip, F. Huang, A. K. Y. Jen, *Adv. Funct. Mater.* **2010**, *20*, 1371; c) S. Chen, J. R. Manders, S. W. Tsang, F. So, *J. Mater. Chem.* **2012**, *22*, 24202.

[4] a) P. M. Beaujuge, J. M. J. Frechet, *J. Am. Chem. Soc.* **2011**, *133*, 20009; b) Y. F. Li, *Acc. Chem. Res.* **2012**, *45*, 723; c) C. J. Brabec, S. Gowrisanker, J. J. M. Halls, D. Laird, S. J. Jia, S. P. Williams, *Adv. Mater.* **2010**, *22*, 3839; d) P. L. T. Boudreault, A. Najari, M. Leclerc, *Chem. Mater.* **2011**, *23*, 456; e) S. C. Price, A. C. Stuart, L. Q. Yang, H. X. Zhou, W. You, *J. Am. Chem. Soc.* **2011**, *133*, 4625; f) E. Wang, Z. Ma, Z. Zhang, K. Vandewal, P. Henriksson, O. Inganas, F. Zhang, M. R. Andersson, *J. Am. Chem. Soc.* **2011**, *133*, 14244; g) H. Zhong, Z. Li, F. Deledalle, E. C. Fregoso, M. Shahid, Z. Fei, C. B. Nielsen, N. Yaacobi-Gross, S. Rossbauer, T. D. Anthopoulos, J. R. Durrant, M. Heeney, *J. Am. Chem. Soc.* **2013**, *135*, 2040.

[5] Z. C. He, C. M. Zhong, S. J. Su, M. Xu, H. B. Wu, Y. Cao, *Nat. Photonics* **2012**, *6*, 591.

[6] a) E. J. Zhou, J. Z. Cong, K. Hashimoto, K. Tajima, *Energy Environ. Sci.* **2012**, *5*, 9756; b) M. C. Scharber, M. Koppe, J. Gao, F. Cordella, M. A. Loi, P. Denk, M. Morana, H. J. Egelhaaf, K. Forberich, G. Dennler, R. Gaudiana, D. Waller, Z. G. Zhu, X. B. Shi, C. J. Brabec, *Adv. Mater.* **2010**, *22*, 367; c) J. C. Bijleveld, A. P. Zoombelt, S. G. J. Mathijssen, M. M. Wienk, M. Turbiez, D. M. de Leeuw, R. A. J. Janssen, *J. Am. Chem. Soc.* **2009**, *131*, 16616; d) D. Muhlbacher, M. Scharber, M. Morana, Z. G. Zhu, D. Waller, R. Gaudiana, C. Brabec, *Adv. Mater.* **2006**, *18*, 2884.

[7] J. Gilot, M. M. Wienk, R. A. J. Janssen, *Adv. Mater.* **2010**, *22*, E67.

[8] a) S. Sista, Z. R. Hong, L. M. Chen, Y. Yang, *Energy Environ. Sci.* **2011**, *4*, 1606; b) T. Ameri, G. Dennler, C. Lungenschmied, C. J. Brabec, *Energy Environ. Sci.* **2009**, *2*, 347; c) J. Y. Kim, K. Lee, N. E. Coates, D. Moses, T. Q. Nguyen, M. Dante, A. J. Heeger, *Science* **2007**, *317*, 222; d) Y. H. Zhou, C. Fuentes-Hernandez, J. W. Shim, T. M. Khan, B. Kippelen, *Energy Environ. Sci.* **2012**, *5*, 9827; e) V. S. Gevaerts, A. Furlan, M. M. Wienk, M. Turbiez, R. A. J. Janssen, *Adv. Mater.* **2012**, *24*, 2130; f) W. Li, A. Furlan, K. H. Hendriks, M. M. Wienk, R. A. J. Janssen, *J. Am. Chem. Soc.* **2013**, *135*, 5529.

[9] G. Dennler, M. C. Scharber, T. Ameri, P. Denk, K. Forberich, C. Waldauf, C. J. Brabec, *Adv. Mater.* **2008**, *20*, 579.

[10] a) J. You, L. Dou, K. Yoshimura, T. Kato, K. Ohya, T. Moriarty, K. Emery, C. C. Chen, J. Gao, G. Li, Y. Yang, *Nat. Commun.* **2013**, *4*, 1446; b) Helitek website, http://www.heliatek.com, accessed: June 2013.

[11] a) W. W. Li, W. S. C. Roelofs, M. M. Wienk, R. A. J. Janssen, *J. Am. Chem. Soc.* **2012**, *134*, 13787; b) L. T. Dou, J. Gao, E. Richard, J. B. You, C. C. Chen, K. C. Cha, Y. J. He, G. Li, Y. Yang, *J. Am. Chem. Soc.* **2012**, *134*, 10071; c) W. Li, K. H. Hendriks, W. S. C. Roelofs, Y. Kim, M. M. Wienk, R. A. J. Janssen, *Adv. Mater.* **2013**, *25*, 3182.

[12] a) L. Ye, S. Q. Zhang, W. Ma, B. H. Fan, X. Guo, Y. Huang, H. Ade, J. H. Hou, *Adv. Mater.* **2012**, *24*, 6335; b) L. T. Dou, J. B. You, J. Yang, C. C. Chen, Y. J. He, S. Murase, T. Moriarty, K. Emery, G. Li, Y. Yang, *Nat. Photonics* **2012**, *6*, 180.

[13] J. C. Bijleveld, V. S. Gevaerts, D. Di Nuzzo, M. Turbiez, S. G. J. Mathijssen, D. M. de Leeuw, M. M. Wienk, R. A. J. Janssen, *Adv. Mater.* **2010**, *22*, E242.

[14] L. T. Dou, W. H. Chang, J. Gao, C. C. Chen, J. B. You, Y. Yang, *Adv. Mater.* **2013**, *25*, 825.

[15] H. Choi, J. S. Park, E. Jeong, G. H. Kim, B. R. Lee, S. O. Kim, M. H. Song, H. Y. Woo, J. Y. Kim, *Adv. Mater.* **2011**, *23*, 2759.

[16] J. Jo, A. Pron, P. Berrouard, W. L. Leong, J. D. Yuen, J. S. Moon, M. Leclerc, A. J. Heeger, *Adv. Energy Mater.* **2012**, *2*, 1397.

[17] a) Y. M. Sun, J. H. Seo, C. J. Takacs, J. Seifter, A. J. Heeger, *Adv. Mater.* **2011**, *23*, 1679; b) W. J. E. Beek, M. M. Wienk, M. Kemerink, X. N. Yang, R. A. J. Janssen, *J. Phys. Chem. B* **2005**, *109*, 9505.

[18] M. M. Beerbom, B. Lagel, A. J. Cascio, B. V. Doran, R. Schlaf, *J. Electron Spectrosc. Relat. Phenom.* **2006**, *152*, 12.

Adv. Mater. **2013**,
DOI: 10.1002/adma.201301288